

Reversible Charge Trapping/Detrapping in a Photoconductive Insulator of Liquid Crystal Zinc Porphyrin

Chong-yang Liu, Horng-long Pan, Marye Anne Fox,* and Allen J. Bard*

Department of Chemistry and Biochemistry, The University of Texas at Austin,
Austin, Texas 78712

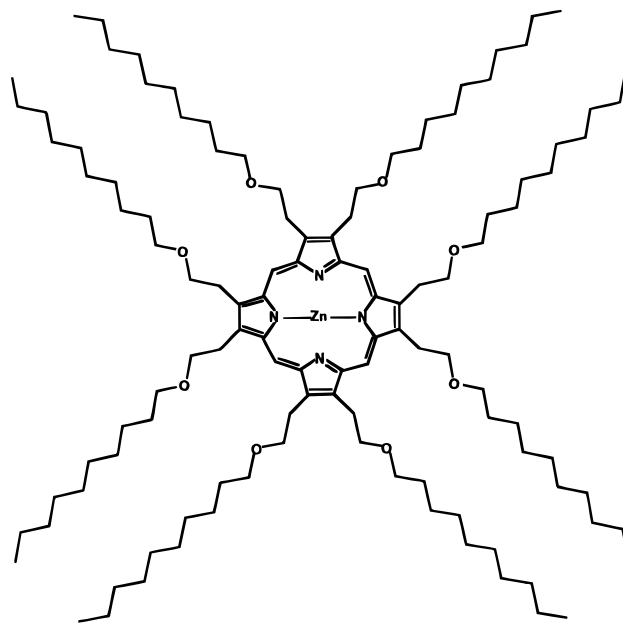
Received January 14, 1997. Revised Manuscript Received April 3, 1997[⊗]

A molecular crystal of zinc octakis(β -decoxyethyl) porphyrin (ZnODEP) is an insulator in the dark and becomes conductive under irradiation. An externally controllable charge trapping and detrapping within ZnODEP thin films ($\sim 1 \mu\text{m}$) occurs when symmetrical sandwich cells of ITO/ZnODEP/ITO are irradiated under a proper bias voltage between two parallel ITO (indium–tin oxide) electrodes. The trapping and detrapping rise time is on the nanosecond time scale. Detrapping of charge stored previously in the cell could be accomplished with pulse irradiation under short-circuit conditions and gives rise to a discharge current spike. Trapped charge induced by a 10 ns laser pulse or by longer time irradiation with a conventional light source could be sensed by a voltage measurement at open circuit. No loss of stored charge was detectable at a 1 pA level for a period of 11 months under open circuit conditions in the dark. After charge trapping with 550 nm light irradiation ($10 \mu\text{W}/\text{cm}^2$) under a bias of 0.5 V, the stored charge induced a voltage difference of ~ 20 mV between the two ITO electrodes. This voltage difference was stable for at least 2000 h with no evidence of decay. These results suggest that ZnODEP as a thin film photoconductive insulator might serve as a memory medium for electrooptical information storage in the form of charge. Such a data storage system would be nonvolatile and rewritable. We have shown that a memory element could be subjected to write (trapping)/erase (detrapping) 1.5 billion times with a readout signal that was essentially identical with the first without any evidence of deterioration. To find attainable resolution, charge was injected with a scanning tunneling microscope tip under different bias. For a 6 V bias, charge was trapped in an element of 40 nm diameter, equivalent to a storage density of 8×10^{10} bits/ cm^2 .

Introduction

We present here experimental evidence of photon excitation-induced charge trapping and detrapping within an organic photoconductive insulator of zinc octakis(β -decoxyethyl)porphyrin (ZnODEP) sandwiched between two plates of optically transparent indium tin oxide (ITO) coated glass. Such charge trapping and detrapping processes occur in an externally controllable manner with light irradiation under a proper bias voltage applied between the two ITO electrodes. We propose ZnODEP as a potential memory medium for information storage. Tests of retention, speed, density, rewritability, and write/read cycle life described here show that thin films of ZnODEP have excellent properties for electrooptical memory.

The ZnODEP molecule, first synthesized by Gregg et al.,¹ has a geometry characterized by a flat aromatic core with eight long alkyl chains, which leads to a crystal structure where the molecules are stacked in columns.² This material has a liquid crystal phase between 95 and 147 °C in which the long hydrocarbon tails become flexible (melt) while the individual molecular columns remain rigid.² ZnODEP was first investigated for use



in photovoltaic devices, where irradiation of solid-state thin-film cells produced photocurrents.^{3,4} In a preliminary communication, we showed that ZnODEP could be

[⊗] Abstract published in *Advance ACS Abstracts*, May 15, 1997.

(1) Gregg, B. A.; Fox, M. A.; Bard, A. J. *J. Am. Chem. Soc.* **1989**, *111*, 3024.

(2) Liu, C.-Y.; Pan, H.-L.; Tang, H.; Fox, M. A.; Bard, A. J. *J. Phys. Chem.* **1995**, *99*, 7632.

(3) Gregg, B. A.; Fox, M. A.; Bard, A. J. *J. Phys. Chem.* **1990**, *94*, 1586.

(4) Gregg, B. A.; Fox, M. A.; Bard, A. J. *J. Phys. Chem.* **1989**, *93*, 4227.

used as a charge storage medium⁵ and had the potential to be used in memory devices.^{6,7}

The properties of light-sensitive substances have been investigated since 1873, when Smith observed the first photoconductivity effect on selenium.⁸ Photoconduction includes the generation (and recombination) of charge carriers and their transport to electrodes. The thermal carrier relaxation process, charge trapping and detrapping processes, charge carrier statistics, electrode effects, and several modes of recombination all contribute to the observed photocurrent.⁹ In addition, impurity-related absorption of subbandgap irradiation may also be important. After over 100 years of investigation, the basic mechanisms of charge generation and transport are reasonably well understood, especially for crystalline inorganic semiconductors. Upon irradiation, photocarrier production takes place by band-to-band transitions, impurity level-to-band transitions, or ionization of donors. The mechanism of the absorption depends on the details of the band structure and can be described quantitatively.¹⁰ The concept of bandgap transitions in the optical absorption process and the creation of free charge carriers can be extended to amorphous semiconductors but does not hold for organic compounds in which charge generation takes place through transitions in molecular orbitals (i.e., from ground state to excited state).⁹ Moreover, recombination and transport mechanisms of the charge carriers are also different in organic molecular crystals,⁹ where the weak van der Waals intermolecular interaction forces produce only slight changes in the electronic structure of molecules upon formation of the solid phase, and the molecules in a crystal are largely isolated with respect to the electron density distribution.^{11,12} Hopping, tunneling, and trapping are often employed to describe charge carrier transport in organic molecular crystals.

Charge trapping is probably the most complicated phenomenon in photoconduction, even for inorganic substances, although various approaches toward treating this problem are available.⁹ Trapping sites are often associated with chemical impurities and crystal defects. In principle, one should be able to identify the nature of impurity-related trapping sites and correlate them with electrical, optical, and spectroscopic behavior through systematic doping of known species into the pure substance. Unfortunately, this approach is not suitable for most organic molecular crystals because it is difficult to purify the starting material to adequate levels.¹³ For example, the impurities may be neutral molecules whose properties (i.e., shape, size, solubility) render them hard to separate from the host material

(e.g., anthracene in phenanthrene), or dopant species may be produced as a consequence of the reactivity of the material. For example, tetracyanoquinodimethane, TCNQ, always forms Na^+TCNQ^- in contact with glassware.¹³ Because of the weak short-range intermolecular forces in organic molecular crystals, impurity molecules may often be incorporated into the lattice with only a small, unfavorable enthalpy due to localized lattice strain around the impurity site offset by a favorable entropy of mixing.¹³ Moreover, structural defects, i.e., disorder, dislocations, twinning, and even strain-induced inclusions of regions of different lattice structure, can occur relatively easily, with minor effects on the lattice energy. Therefore, full characterization of the nature, concentration, and distribution of the impurities and defects that can serve as trapping sites is rarely carried out,^{9,13} although suitable methods do exist for such characterization in many materials.

The complexity of the charge trapping process does not prevent its practical applications. For example, visible light emission has been achieved from some large bandgap semiconductors such as GaN, GaP, and SiC by doping of proper elements (i.e., Cd, N, Al, or B) to form suitable trapping levels within the gap.¹⁴ Si_3N_4 based charge trapping devices have been used for many years, although the trapping mechanism is still not fully understood.¹⁵⁻¹⁷ Charge trapping is also fundamental in electrophotography.¹⁸

Experimental Section

ZnODEP was synthesized according to a previously described method¹ and was purified by repeated chromatography on silica gel with a mixture of dichloromethane and ethyl acetate, followed by recrystallization twice from a dichloromethane-methanol and a benzene-methanol mixture. Purity was checked by monitoring absorption, emission, and excitation spectra for adventitious bands. Solvents were spectral grade and were used as received. Octadecyltrichlorosilane (Aldrich) was vacuum distilled prior to use. The results obtained with ZnODEP synthesized in different batches were reproducible. ITO/ZnODEP/ITO symmetrical sandwich cells were prepared by capillary filling^{2,3,19} of ZnODEP in its molten state between two parallel ITO plates separated by about 2–3 μm ; this thickness was determined by the interference pattern. The area of the cells is about 0.3–0.8 cm^2 .

A 250 W Xe lamp (Oriel) was used as an excitation source in the steady-state measurements. For monochromatic irradiation (550 nm), an Oriel monochromator and a cutoff filter (>530 nm) were used. The light intensity was about 5×10^{12} photons $\text{cm}^{-2} \text{s}^{-1}$. Photocurrent measurements were performed with a Princeton Applied Research, Model 175 universal programmer, a Model 173 potentiostat, and a Kipp & Zonen BD 91 recorder.

Nanosecond irradiation was carried out at the Center for Fast Kinetics Research (University of Texas) with the second harmonic (532 nm, 10 ns pulse) of a Quantel YG481 Q-switched Nd:YAG laser. The beam energy was attenuated as necessary by using calibrated metal screens to prevent damage of ITO/ZnODEP/ITO cells. An Orion Reassert Model 710A/digital analyzer was employed for the measurement of voltage.

(5) Liu, C.-Y.; Pan, H.-L.; Fox, M. A.; Bard, A. J. *Science* **1993**, *261*, 897.

(6) Liu, C.-Y.; Pan, H.-L.; Bard, A. J.; Fox, M. A. U.S. Patent 5,327,373.

(7) Liu, C.-Y.; Hasty, T.; Bard, A. J. *J. Electrochem. Soc.* **1996**, *143*, 1916.

(8) Smith, W. *Nature* **1873**, *7*, 303.

(9) Joshi, N. V. *Photoconductivity, Art, Science, and Technology*; Marcel Dekker: New York, 1990.

(10) Pankove, J. I. *Optical Processes in Semiconductors*; Dover: New York, 1975.

(11) Silinsh, E. A.; Capek, V. *Organic Molecular Crystals: Interaction, Localization, and Transport Phenomena*; American Institute of Physics: New York, 1994.

(12) Silinsh, E. A. *Organic Molecular Crystals: Their Electronic States*; Springer-Verlag: Berlin, 1980.

(13) Wright, J. D. *Molecular Crystals*, 2nd ed.; Cambridge University Press: Cambridge, U.K., 1987.

(14) Seeger, K. *Semiconductor Physics*; Springer-Verlag: New York, 1973.

(15) Prince, B. *Semiconductor Memories*, 2nd ed.; John Wiley & Sons: New York, 1991.

(16) Sze, S. M. *Physics of Semiconductor Devices*, 2nd ed.; John Wiley & Sons: New York, 1981.

(17) Chang, J. J. *Proc. IEEE* **1976**, *64*, 1039.

(18) Schein, L. B. *Electrophotography and Development Physics*; Springer-Verlag: Berlin, 1988.

(19) Liu, C.-Y.; Tang, H.; Bard, A. J. *J. Phys. Chem.* **1996**, *100*, 3587.

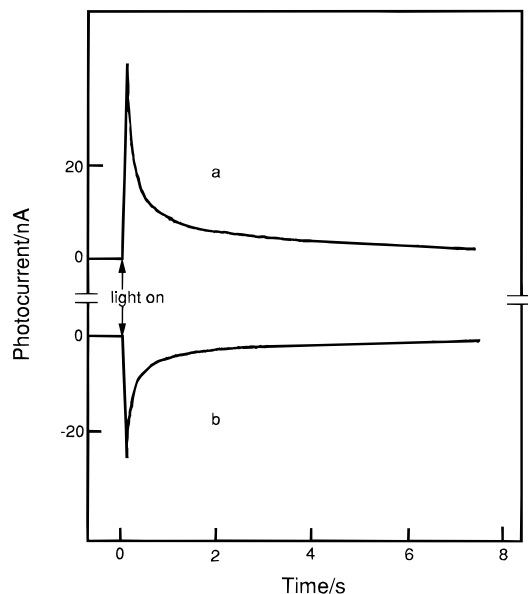


Figure 1. Short-circuit photocurrent of an ITO/ZnODEP/ITO cell as a function of time with a constant irradiation of 550 nm light after irradiation of the cell with a 550 nm light beam under a bias of (a) -2 or (b) $+2$ V for 5 s followed by a rest period of 10 s under short-circuit conditions in the dark.

Results and Discussion

Charge Trapping and Detrapping in ZnODEP.

The porphyrin crystal, like many other organic solids, is an electrical insulator in the dark. The electrical characteristics of organic molecular crystals are generally interpreted in terms of poor overlap between the orbitals of neighboring molecules.¹³ X-ray diffraction of porphyrin crystals shows that the smallest molecule-to-molecule separation is as large as 3.98 \AA ,² so charge cannot pass rapidly from molecule to molecule. Moreover, the porphyrin used in this study was not intentionally doped and therefore contained very few charge-producing species that contribute to electric conduction. Under irradiation, however, the porphyrin molecular crystal becomes conductive due to charge production by photon excitation. A steady-state short-circuit photocurrent was established when ITO/ZnODEP/ITO symmetrical sandwich cells were illuminated without bias, and the photocurrent dropped quickly to zero after irradiation ceased. As discussed in earlier publications, this photocurrent represents injection of electrons into the illuminated (front) ITO electrode and will be denoted as an anodic photocurrent. When the light beam was periodically chopped (5 Hz), the short-circuit photocurrent followed the light and appeared as a square wave. This was also true for photocurrent generated under a small bias voltage (i.e., <1 V) applied to the porphyrin cells. The same response was observed with other porphyrin based crystals.^{3,19}

In contrast, a clear short-circuit photocurrent spike was seen with an ITO/ZnODEP/ITO cell that had been previously exposed to irradiation for 5 s under a bias as shown in Figure 1. In this case, curve a was obtained by irradiating the ITO/ZnODEP/ITO cell at 550 nm under short-circuit conditions after the cell had been illuminated with the same 550 nm light source for 5 s under a bias potential of -2 V followed by a dark period of 10 s at short circuit. In all of the following discussions, the sign of the applied potential is that of the

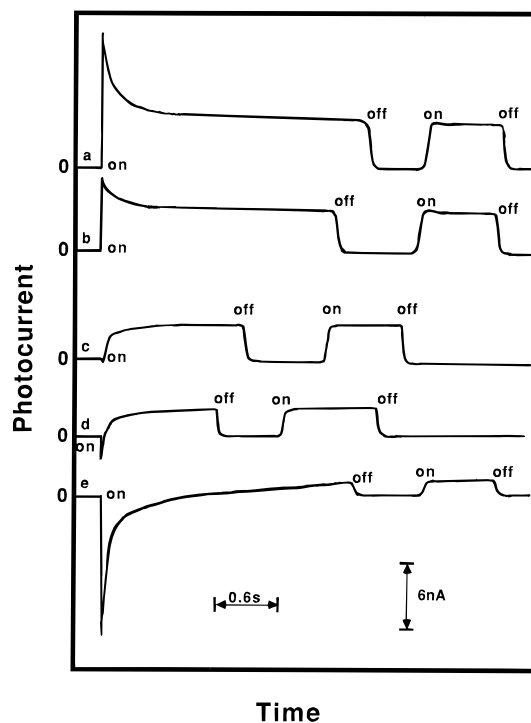


Figure 2. Photocurrent of an ITO/ZnODEP/ITO cell as a function of irradiation (550 nm) time under short-circuit conditions after irradiation of the cell with a 550 nm light under a bias of (a) -0.2 , (b) -0.05 , (c) $+0.2$, (d) $+0.4$, and (e) $+1.2$ V for 5 s and a rest period of 10 s in the dark under short-circuit conditions. On and off indicate the irradiation is turned on and off.

irradiated (or front) ITO electrode with respect to the back electrode. Similarly, a cathodic short-circuit photocurrent spike (curve b) was generated with 550 nm light at short circuit after the cell had been exposed to 550 nm light for 5 s at a bias of $+2$ V and then short-circuited in the dark for 10 s. The magnitude and the direction of the short-circuit photocurrent spikes (anodic or cathodic) were determined by the magnitude and the sign of the bias voltage applied to the cells during the previous irradiation. Such a dependence of the short-circuit photocurrent spike on bias potential during preirradiation suggests that the porphyrin cells were charged during irradiation under bias and were subsequently discharged with irradiation at short-circuit. However, the ITO/ZnODEP/ITO cells do not behave as conventional capacitors, i.e., with porphyrin film acting only as a dielectric material, since the ITO/ZnODEP/ITO cells do not discharge at short circuit in the dark. Thus the charge stored during irradiation under bias is not stored on the two conductor (ITO) surfaces.

To explore the charge/discharge phenomena, the relationship between the size of the discharge current spike and bias voltage applied to the cells during the charge process was systematically investigated. The evolution of a short-circuit photocurrent spike from anodic to cathodic as a function of bias is shown in Figure 2. Curves a–e were obtained with the same sample under identical discharge conditions (i.e., irradiation with 550 nm light at short circuit) after the cell had been short-circuited for 10 s in dark. The anodic discharge current spike decreases from curve a to b. A cathodic spike begins to appear in curve c and increases significantly in curves d and e. In all cases, after the transient dies away, the current settles to the

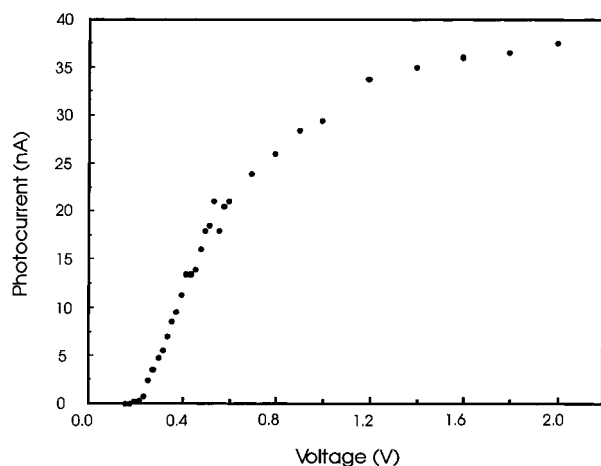


Figure 3. Short-circuit cathodic photodischarge current spike maximum as a function of bias voltage applied in previous charging for 5 s with 550 nm light irradiation.

steady-state anodic photocurrent as long as the cell is illuminated. The short-circuit photocurrent spike was seen only on initial irradiation for all five curves. Then the photocurrent as a function of time follows the on-off square wave behavior that is always observed with a normal uncharged ITO/ZnODEP/ITO cell. Note that the light beam was manually chopped on and off in these measurements and thus the rise time could not be determined. As discussed later, the rise time of the photocurrent of ITO/ZnODEP/ITO cells is in the subnanosecond regime.³

The magnitude of steady-state short-circuit photocurrent appears different for the five curves shown in Figure 2, because a complete discharge was not fully accomplished during the period shown. After a longer period of irradiation, however, the steady-state photocurrent did reach the same magnitude; i.e., the cell was fully recovered to its uncharged state. In general, under the same irradiation, a higher bias voltage during charging produced a larger stored charge.

The curves shown in Figure 2 can thus be taken as the sum of two components: the transient discharge current and the steady-state short-circuit photocurrent. In curves c, d, and e, the discharge current is in the opposite direction from the steady-state photocurrent, so the initial cathodic transient current spikes shifted to the anodic steady-state current as the stored charges were depleted.

An important distinction in comparing the cell to a conventional capacitor is that irradiation is always involved for both charge and discharge processes in ITO/ZnODEP/ITO cells. This clearly indicates that charges are stored within the photoconductive insulator of the ZnODEP layer rather than on the two ITO surfaces and therefore no discharge occurs under short-circuit conditions in the dark. Trapping of charge on crystal defects, grain boundaries, and chemical impurities within the ZnODEP layer are probably responsible for the charge storage in this system. This conclusion was further confirmed by the dependence of the magnitude of discharge photocurrent spike on the bias voltage applied to ITO/ZnODEP/ITO cells for charging as shown in Figure 3. The discharge photocurrent strongly increased with bias voltages from 0 to 1.2 V and then leveled off at higher voltages. This suggests that once the deep traps were fully occupied, a further increase

in the bias voltage makes no large difference in charging. This is in contrast to conventional capacitors where charge and discharge always depend linearly on the magnitude of applied bias (until the breakdown of dielectric material).

Charge trapping processes are often associated with crystal defects and chemical impurities. For example, defects in a molecular crystal may perturb the local electronic configuration leading to a trapping state, since the lattice may be expanded or compressed depending on the type of the structural defects.²⁰ An impurity molecule that replaces a host molecule in an organic crystal, by virtue of its different shape and electronic structure, will interact with neighboring molecules of the host lattice in a different manner than the interactions between host molecules. This will disrupt the electronic structure associated with the regular lattice periodicity. Impurities with vacant orbitals lower in energy than those of the host molecules will be energetically favored sites for electron trapping. Impurities which occupy the interstitial sites will have a similar effect; impurity molecules with a high electron affinity will accept electrons and act as trapping sites.¹³

In an organic molecular crystal, impurities are often incorporated into a crystal near dislocations where the lattice is terminated. On the other hand, impurities may favor the formation of dislocations: when molecules of different size are incorporated into organic solids, an increased density of dislocations may be observed.²¹ Even carefully purified and grown molecular crystals inevitably contain a considerable level of residual impurities and defects compared to inorganic materials such as silicon. Therefore, charge trapping is a general characteristic of organic molecular crystals. This trapping suggests that the photoconductive insulator of ZnODEP could find application as a memory medium based on its capability of reversible charge trapping and detrapping.

Potential Application of ZnODEP as a Memory Medium. The principle of a proposed memory device using a photoconductive insulator like ZnODEP is illustrated in Figure 4. Irradiation of the device with a write beam (550 nm) of sufficient energy to excite the ground state of ZnODEP to its first singlet state gives rise to a cathodic photocurrent when a negative potential is applied to the irradiated ITO with respect to the other ITO electrode. During the writing step, traps within the film are filled with electrons (Figure 4A). These traps have the capacity to store electrons and to release them under appropriate conditions. Electron movement can be prevented and the memory frozen by switching off the light, leaving the material in the insulator state. In the dark, charge remains stored under both open-circuit and short-circuit conditions. The written information can be read out by irradiation of the device with a read beam (550 nm) under short-circuit conditions, causing release of electrons from the traps producing an anodic photocurrent spike as shown in Figure 4A. In an analogous way, one can remove electrons from the traps (inject holes) with a write beam under a positive potential bias, as illustrated in Figure

(20) Simon, J.; Andre, J.-J. *Molecular Semiconductors, Photoelectrical Properties and Solar Cells*; Springer-Verlag: Berlin, 1985.

(21) Meier, H. *Organic Semiconductors: Dark- and Photoconductivity of Organic Solids*; Verlag Chemie: Weinheim, Germany, 1974.

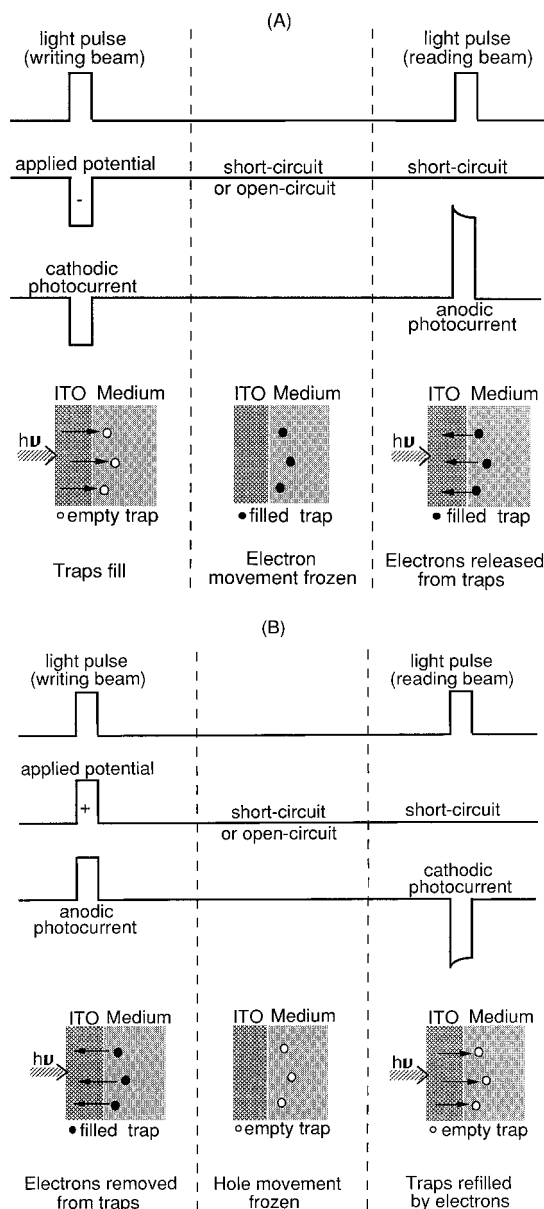


Figure 4. Principle of an electrooptical memory device based on a photoinduced charge trapping and detrapping processes. (A) Under negative bias, the write beam causes electron storage at trap sites. The electrons stored can be released by a read beam under short-circuit conditions. (B) Under positive bias, the write beam leads to depopulation of trap sites (hole storage). The vacancies can be refilled with electrons by a read beam under short-circuit conditions.

4B. These trapped holes can be frozen in the dark at open or short circuit. Again, the stored information can be released with a read beam without bias. A cathodic photocurrent spike is generated as a result of trap refilling. An alternative approach to reading the stored charge was to measure the potential across the cell at open circuit (i.e., with a high impedance voltmeter) in the dark, as discussed later.

In considering this as a memory device, either the anodic or cathodic photocurrent spikes shown in Figure 4 can be taken to represent the memory state, 1, compared to an uncharged, 0, state. Alternatively, this can be the basis of a unique three-state device. The magnitude of the read current spikes depended on the wavelength, light intensity, pulse width of the write beam, and magnitude of potential bias. It was not

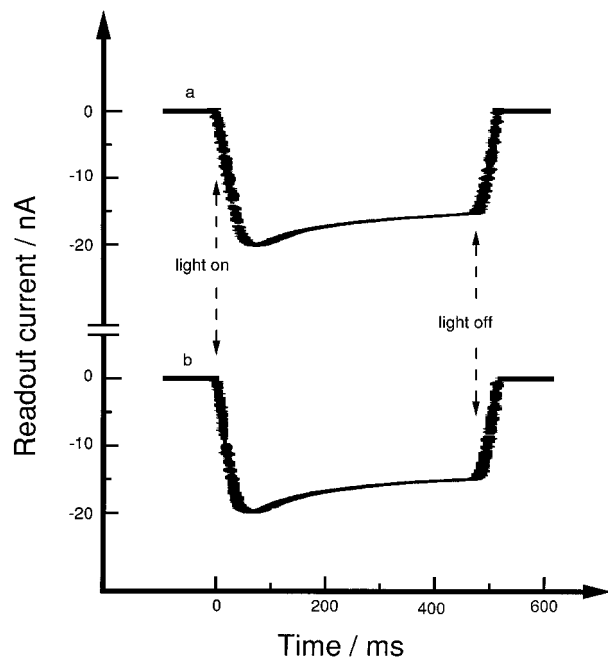


Figure 5. Readout current pulses with the same writing conditions (+0.5 V for 500 ms): (a) initial readout and (b) after 1.5 billion write/erase cycles.

necessary for the light pulse and potential pulse to be precisely synchronized in the write step, so long as the bias was maintained for the duration of the photocharging event. In fact, a longer potential pulse did not make any difference in the amount of stored charge, because of the insulating property of ZnODEP in the dark.

We now address a number of key factors in these devices. The duration of charge retention in the ITO/ZnODEP/ITO cells was very long. In an actual measurement, no loss of stored charge was detectable at the picoampere level for a period of 11 months under open circuit conditions in the dark. An even longer retention time is probable; e.g., charges stored in Si_3N_4 remain trapped for many years.¹⁶ We also tested the number of trap/detrapping cycles possible. In this case, the cycle life was tested by applying continuous potential pulses of 0 to +0.5 V with a pulse width and interval of 500 ms to the cell with constant irradiation. Under these conditions, the memory element was charged at +0.5 V and was immediately followed by a readout at 0 V. The readout current was the same for continuous cycling for 82 days. The test was then carried out with 1 ms pulses. Again, the output current of each reading was essentially identical after the cell had been subjected to 1.5 billion read/refresh cycles. When the potential pulse was readjusted to 500 ms, the readout signal was the same as the first shown in Figure 5. The remarkable cycle life, greater than 1.5 billion cycles, indicates that the charge storage process does not involve any chemical changes, structural transitions, or phase changes. Charge (either electrons or holes) is simply transferred to or from preexisting traps that do not change over time during the charge/discharge process. This implies that there should be no irreversible changes during extended cycling, which is important for a practical device.

When the device was read out in terms of photocurrent, the amount of charge remaining in the traps was reduced after each reading. However, many readings could be made before the traps were completely de-

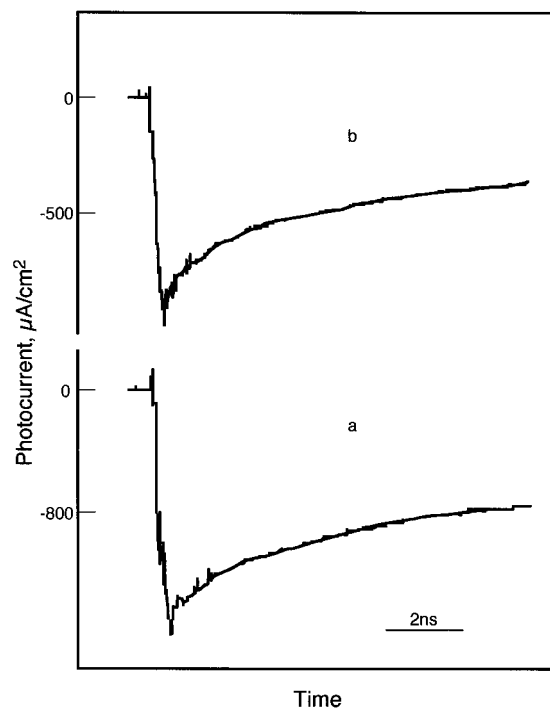


Figure 6. Readout photodischarge current as a function of time under short-circuit conditions (after charging at 1 V for 10 ns) for the (a) first and (b) 1532nd 10 ns laser pulse (read beam).

pleted, as shown in Figure 6. In this case, the cell was charged under a bias of 1 V with 550 nm light for 10 ns and was then discharged consecutively at short circuit with a series of 10 ns laser pulses. The interval between the pulses was 1 s in the dark. The first and the 1532nd photodischarge currents as a function of time are shown in Figure 6. The read rise time was well below 1 ns and the readout current after 1532 pulses was still over 60% of the initial readout signal. It is also possible to refresh the cell after readout, as with dynamic RAMs. As shown in Figure 7, one could set a potential pulse with the proper width and magnitude to the memory element coupled with the reading beam pulse. The first part of the reading beam pulse causes a photodischarge under short circuit conditions, while during the second part of the reading beam, a potential pulse is applied to recharge the memory element. In this case, the memory element is refreshed once after each reading.

Readout can also be implemented by measuring the voltage produced by the photoinduced charge storage in the dark. An actual measurement of the readout voltage is shown in Figure 8, which was obtained after the storage of charge by writing with a 10 ns laser pulse. Note that a negative voltage of -280 mV was generated with a -1.0 V bias during writing (Figure 8a), and a positive voltage of $+200$ mV was induced under a $+1.0$ V bias (Figure 8b). Since no charge flows during voltage measurement, depletion of the signal charge does not occur in this reading mode. Compared to the transient photocurrent measurement shown in Figure 1, the readout voltage is essentially constant over time (Figure 8). This result also shows that the operation speed in the ITO/ZnODEP/ITO cells was in the nanosecond regime; i.e., information could be written into this medium with a 10 ns laser pulse and could be read out as a dark potential or as a 10 ns pulse as discussed previously.³ A long-term experiment was performed to

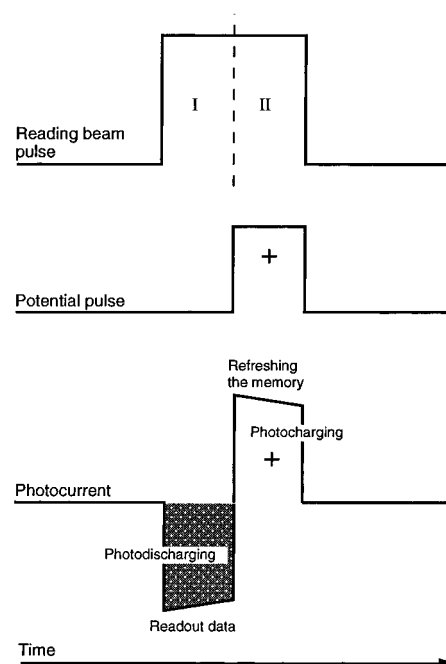


Figure 7. Method for refreshing memory. A reading beam pulse is coupled with a potential pulse such that the stored data is read out (i.e., photodischarged under zero bias) with the first part of the reading beam pulse. A potential pulse is coincidentally applied with the second part of the reading beam pulse so that the memory cell is refreshed (i.e., photocharged under bias) immediately after the readout.

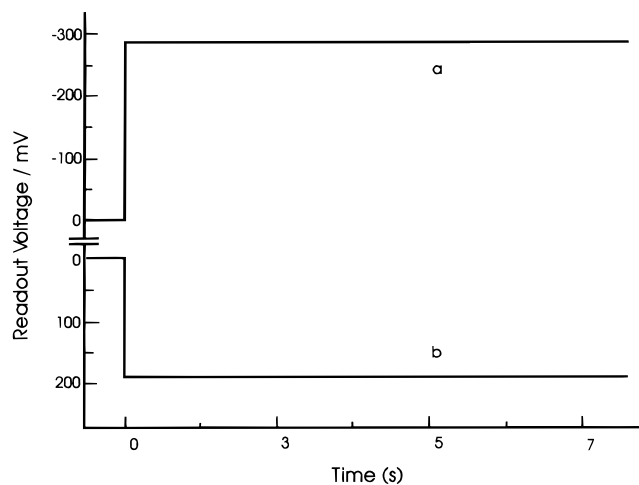


Figure 8. Readout voltage as a function of time. The data were stored by a single 10 ns laser pulse irradiation under a potential of (a) -1.0 and (b) $+1.0$ V.

identify the extent to which the readout is nondestructive. The charge was generated and stored by a low-intensity writing beam (ca. $10 \mu\text{W}/\text{cm}^2$) under a small bias ($+0.5$ V), and the stored charge was read out continuously for over 2000 h. The readout voltage was quite constant with no evidence of decay, as shown in Figure 9.

Spatial Resolution—Charge and Discharge at Tip. To estimate the data storage density with the proposed memory medium, a sharp Pt–Ir scanning tunneling microscopy (STM) tip was employed as a liftable electrode to charge and discharge a ZnODEP thin film ($\sim 250 \mu\text{m}$). The use of an STM tip for studies of a memory medium was first introduced by Barrett and Quate,²² who monitored capacitance at an Si_3N_4 surface on which charge was deposited. Since the STM

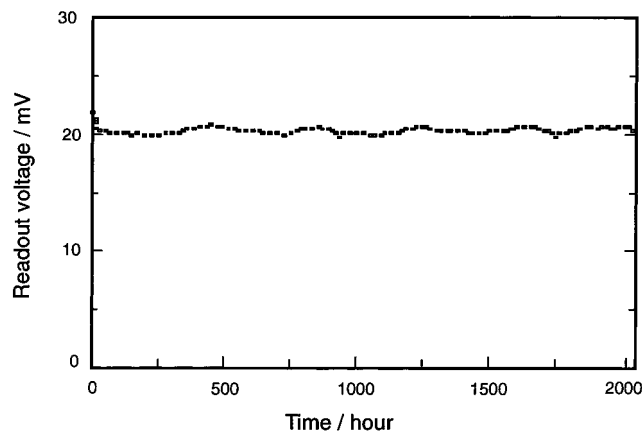


Figure 9. Readout voltage as a function of time, demonstrating the nondestructive nature of the readout operation. The data were stored by a low level write beam (ca. $10 \mu\text{W}/\text{cm}^2$) under a bias of +0.5 V.

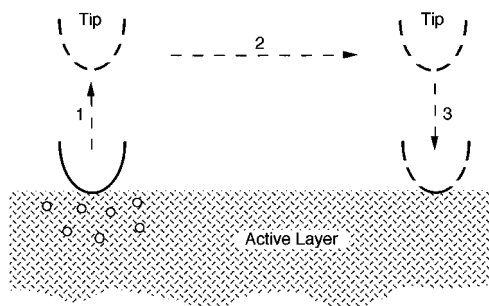


Figure 10. Schematic diagram of the procedure used to estimate the size of an individual memory element with an STM tip.

tip could be made extremely sharp, a very small spot could be probed. In this case, the ITO/ZnODEP/ITO sandwich cell was separated so that one surface of the organic layer was exposed. The tip was then brought into contact with the film to form the structure ITO/ZnODEP/tip (Figure 10). The tip could be moved both perpendicularly and parallel relative to the film surface. The sample could be charged and discharged with the tip following the same procedures as described above. This configuration was used to determine the extent the charges stored under the tip spread parallel to the film surface. This determines the minimum size of an individual pixel and therefore the data storage density. As shown in Figure 10, once a particular spot, a, was charged at a given bias, the tip was moved to a nearby spot, b, to determine a zero bias discharge current at the new tip position. Since no charges were previously stored at site b, any discharge current observed reflects the movement of charge (cross talk) between these two sites. By systematically varying the distance, a critical distance from the charged spot was found where essentially no discharge current was detectable. This represented the maximum lateral size of the individual memory element under the given bias and irradiation conditions. Note that the addressing laser beam diameter is much larger than the stored charge site, since charging and spatial resolution is governed by the electric field under the tip.

The reliability of this method was confirmed by a number of experiments. For example, after several

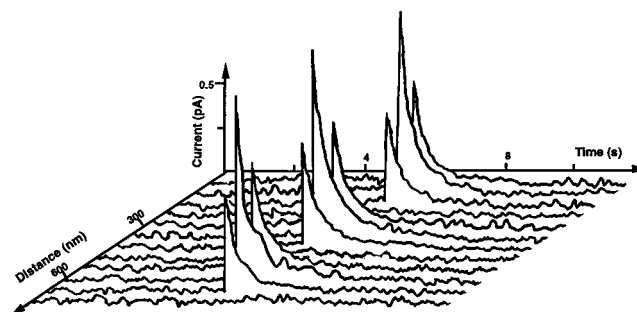


Figure 11. Discharge current as a function of time and distance. Charges were stored under a bias of 10 V.

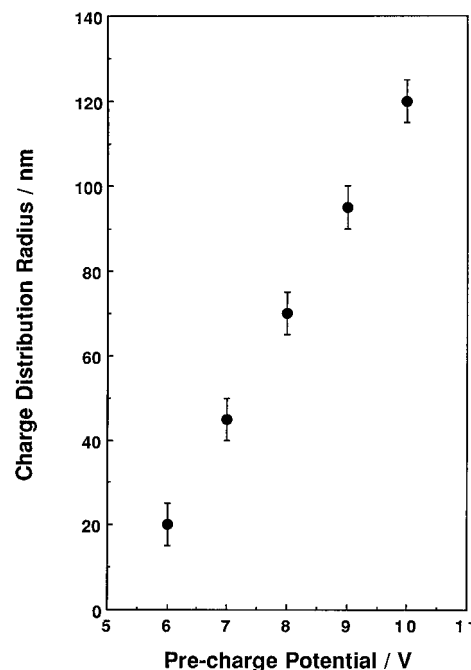


Figure 12. Horizontal charge distribution radius as a function of precharge potential.

attempted discharges at site b were carried out, the tip was moved back to its original position (site a) and the discharge current was observed. In this case, charge was preserved at site a, since none of the charge stored was released with the tip at site b; therefore, measurements at a remote site caused essentially no disturbance to the charges stored at site a. To test that the tip was really in good contact with the memory medium at site b, charge/discharge cycles were sometimes carried out. When the tip was positioned somewhere within the critical distance, the discharge current was of smaller magnitude than that found at the charged site. Thus, the charge was highly localized, with no communication among isolated trapping sites. A full discharge could only be made at exactly the same position of site a.

A three-dimensional plot of discharge current under a bias of 10 V as a function of time and distance is shown in Figure 11 for three adjacent pixels within a ZnODEP film. These three storage sites were totally independent of each other across a distance of less than 750 nm. When a smaller bias was used, less charge was stored and the size of the elementary memory cell was even smaller. The size of the individual storage unit as a function of bias, shown in Figure 12, indicates that the horizontal charge distribution radius decreases with bias voltage. For example, when a spot was charged

under a bias of 6 V, the pixel was 40 nm in diameter, corresponding to a storage density of $\sim 8 \times 10^{10}/\text{cm}^2$.

Conclusions

The localization or isolation of trapped charges is crucial for high-density data storage. Organic substances should have an inherent advantage over inorganic materials, since most organic molecular crystals are made of discrete molecules that preserve their individual identity.^{11,12} For example, the crystal spectrum retains the spectral features of individual molecules, including their electronic-vibrational structure. The charge carriers are mainly localized on individual molecules and move only by hopping from one molecule to another in the organic crystals. These crystals often exhibit poor overlap between orbitals of neighboring molecules and are electric insulators in the dark.¹¹⁻¹³ In terms of electronic configuration, organic molecular crystals are considered as being closer to an oriented molecular gas than to a usual inorganic crystal with a strongly bonded rigid atomic or ionic lattice characterized by complete loss of individual properties of the constituent atoms in the crystal.¹² Moreover, the ZnODEP crystal used here has an additional unique structural feature, because the flat molecules are stacked one on top of another to form well-ordered individual molecular columns that are insulated from one another by long hydrocarbon chains.² Because the intercolumn separation is as large as 24 \AA ,² charges trapped in neighboring molecular columns do not communicate with each other. Such a quasi-one-dimensional molecular crystal is therefore a good charge trapping material for high-density data storage. In principle, the theoretical size of one memory element could be a single molecular column representing the ultimate density in information storage. This can only be realized, however, when practical difficulties, including the sensitivity of the detection system and means of addressing an element, can be overcome.

At present, the compact disk (CD), a read only memory, represents the highest density commercial data storage. There are now large efforts under way to

develop rewritable disks for information storage. One promising recording technology is based on phase changes in the active layer,²³⁻²⁶ i.e., a change between crystalline and amorphous or microcrystalline states in a metal film. The film is initially crystalline, with a high reflectivity. A short pulse of laser beam heats the memory element and allows it to cool with either much smaller crystals or in an amorphous form, which has a lower reflectivity. The stored data are erased by heating the signal element again above its melting point, just as in recording, but allowing it to cool more slowly so that a crystalline structure can develop. The key problem in this method is that material fatigue effects limit the number of times any element can be erased and rewritten. A similar problem also exists in another method, thermoplastic recording,²⁶ where the writing laser beam softens a dye-polymer layer and leaves a pit, which is smoothed out by heating a large area in erasing. Both of these methods have a spatial resolution limited by the wavelength of the laser beam. This cycling problem, however, does not appear to be a concern in ZnODEP, in which no physical change is required for data writing and erasing, and no evidence of deterioration was seen even after 1.5 billion cycles. The resolution of storage, as demonstrated in the STM tip experiments, is governed by the electric field not the irradiation. In addition, high speed, high density, and low cost make ZnODEP a very attractive memory medium for information storage.

Acknowledgment. The support of this research by the Texas Advanced Research Program, the National Science Foundation (CHE9423874), and the Robert A. Welch Foundation is gratefully acknowledged.

CM970039B

(23) Feinleib, J.; de Neufvill, J.; Moss, S. C.; Ovshinsky, S. R. *Appl. Phys. Lett.* **1971**, *18*, 254.

(24) Bell, A. E.; Spong, F. W. *Appl. Phys. Lett.* **1981**, *38*, 920.

(25) Chen, M.; Rubin, K. A.; Barton, R. W. *Appl. Phys. Lett.* **1986**, *49*, 502.

(26) Bradley, A. *Optical Storage for Computers, Technology and Applications*; Ellis Horwood: New York, 1989.